Original article

The Effect of Parallel-hole Collimator Material on Image and Functional Parameters in SPECT Imaging: A SIMIND Monte Carlo Study

Ahmadreza Azarm, Jalil Pirayesh Islamian, Babak Mahmoudian[1], Esmaeil Gharepapagh[1]

Department of Medical Physics, Faculty of Medicine, [1]Nuclear Medicine Unit, Department of Radiology, Faculty of Medicine, Tabriz University of Medical Sciences, Tabriz, Iran

Abstract

The collimator in single-photon emission computed tomography (SPECT) is a critical component of the imaging system and plays an impressive role in the imaging quality. In this study, the effect of the collimator material on the radioisotopic image and its functional parameters was studied. The simulating medical imaging nuclear detectors (SIMIND) Monte Carlo program was used to simulate a Siemens E.CAM SPECT (Siemens Medical Solutions, Erlangen, Germany) system equipped with a low-energy high-resolution (LEHR) collimator. The simulation and experimental data from the SPECT imaging modality using ^{99m}Tc were obtained on a point source and Jaszczak phantom. Seventeen high atomic number materials were considered as LEHR collimator materials. In order to determine the effect of the collimator material on the image and functional parameters, the energy resolution, spatial resolution, contrast, and collimator characteristics parameters such as septal penetration and scatter-to-primary ratio were investigated. Energy spectra profiles, full width at half maximums (FWHMs) (mm) of the point spread function (PSF) curves, system sensitivity, and contrast of cold spheres of the Jaszczak phantom for the simulated and experiment systems have acceptability superimposed. The results of FWHM and energy resolution for the 17 collimators showed that the collimator made of 98% lead and 2% antimony could provide the best FWHM and energy resolution, 7.68 mm and 9.87%, respectively. The LEHR collimator with 98% lead and 2% antimony offers the best resolution and contrast when compared to other high atomic number metals and alloys.

Keywords: Collimator material, functional parameters, image quality, Monte Carlo simulation, single-photon emission computed tomography, simulating medical imaging nuclear detectors

Introduction

Single-photon emission computed tomography (SPECT) is a nuclear medicine tomographic imaging modality. SPECT is a powerful tool for quantifying the three-dimensional distribution of a radiotracer in humans, especially in oncology. SPECT is considered to be the preferred modality in studying functional abnormalities between normal and cancer cells.[1-4] In this process, the gamma rays from the administered radioisotope are encountered with photon attenuation and scattering. The gamma rays, before collision with the detector, encountered the collimator. The quality of the images in SPECT is seriously affected by the collimator's structure, properties of the detector, reconstruction algorithms, and also attenuation/scattering of gamma rays in the patient's body and the collimator.[5-8] The collimation system is a critical component of a SPECT imaging system. Performance of a collimator was improved by increasing the absorption efficiency of the collimator material.[9-11] Since nuclear medicine imaging deals with random phenomena such as radioactive decay and detection of photons, the Monte Carlo simulation is a suitable tool in nuclear medicine imaging. The purpose of the current study is to evaluate the effect of the parallel-hole collimator material for a low-energy

Access this article online

Quick Response Code:

Website: www.wjnm.org

DOI: 10.4103/1450-1147.163242

Address for correspondence:
Dr. Jalil Pirayesh Islamian, Department of Medical Physics, School of Medicine, Tabriz University of Medical Sciences, Attar Neyshapouri Street, Azadi Avenue, Tabriz - 5166614766, Iran. E-mail: pirayeshej@gmail.com

high-resolution (LEHR) collimator on the image and system parameters.

Materials and Methods

In the present study, 17 materials were considered as LEHR collimator materials [Table 1]. These components and alloys have a high atomic number and linear attenuation coefficient, so they provide high-absorption efficiencies for gamma rays.[12] The Siemens E.CAM gamma camera equipped with two removable SE-LEHR (Siemens Medical Solutions, Erlangen, Germany) collimators was simulated by the simulating medical imaging nuclear detectors (SIMIND, Developed by Professor Michael Ljungberg, sweden) Monte Carlo simulation program version 5.0, which is well established for SPECT imaging.[5,13-15] A 1.5 mm ^{99m}Tc point source (3.7 MBq) and a Jaszczak Deluxe ECT phantom (model ECT/DLX/P) filled with water and 370 MBq activity of ^{99m}Tc were used for the experiment and simulated systems.[16] The energy resolution, spatial resolution, image contrast, and system sensitivity as a function of the collimator materials were determined according to the established and published quality control tests.[17,18] Spatial and energy resolutions were determined by placing a ^{99m}Tc point source at the center of the field of view (FOV), at 10 cm from the collimator surface for both the systems and the planar images were acquired in matrices of 128 × 128 pixels, 0.27 mm pixel size, and 10 million counts for the systems. The sensitivities were determined by the ratio of the detected counts per second per unit activity (cps/MBq) for a point source placed at 25 cm from the detector surface and 10 million photons were detected. The Jaszczak Deluxe ECT phantom was also employed to calculate the image quality, and measurements were acquired experimentally and also by simulation. The phantom was positioned at 15 cm from the collimator surface and the projections along the axis of rotation were acquired in matrices of 128 × 128 pixels, 128 views, 360° clockwise rotation, 1.23 zoom factor, 0.39 mm pixel size, and 1 million counts/projection. The system setup for Jaszczak scanning is shown in Figure 1. The projections were obtained within the 15% energy window width centered on the ^{99m}Tc photopeak. The images were reconstructed by the filtered back projection (FBP) using a ramp combined with a Butterworth filter of order 5 and cutoff frequency of 0.25 cycles/cm. Spatial resolution (in mm) was determined by the smallest visible rods in the reconstructed images.

Results and Discussion

Figure 2 shows the normalized energy spectra from the experiment and simulated gamma cameras for a ^{99m}Tc point source scanning. Energy spectra profiles of the systems have acceptability superimposed.

The calculated energy resolutions for the 140 keV photopeak within 15% windows obtained for simulation and experiment were 10.14% and 10.13%, respectively. The full width at half maximums (FWHMs) of point spread function (PSF) curves for the 10 cm source to collimator distance were determined to be 7.74 mm for both the systems; also, the sensitivities were calculated to be 74.76 cps/MBq and 74.90 cps/MBq, respectively. The qualities of the images were compared in terms of the contrast and spatial resolution obtained by images of the cold spheres and cold rods in the Jaszczak phantom.[19] The results of image contrast for the phantom obtained from simulation and also by experiment were calculated by Equation 1 and the data are shown in Table 2.

Table 1: The percentage of metals and alloys that were used as the collimator material for a SPECT imaging system

Collimator material	Percentage of components
Lead	Pb (100)
Lead antimony (1)	Pb (98), Sb (2)
Lead antimony (2)	Pb (97), Sb (3)
Lichtenberg's metal	Bi (50), Pb (30), Sn (20)
Newton's metal	Bi (50), Pb (31), Sn (19)
Rose's metal	Bi (50), Pb (28), Sn (22)
D'Areet's metal	Bi (50), Pb (25), Sn (25)
Solder 1	Pb (50), Sn (37.5), Bi (12.5)
Solder 2	Sn (50), Bi (25), Pb (25)
Malotle's metal	Bi (46), Sn (34), Pb (20)
Lipowitz metal (cerrobend)	Bi (50), Pb (27), Sn (13), Cd (10)
Wood's metal	Bi (50), Pb (25), Sn (12.5), Cd (12.5)
Ternary eutectic	Bi (56), Sn (40), Zn (4)
Lead tungsten	Pb (98), W (2)
Platinum	Pt (100)
Platinum-cobalt	Pt (77), Co (23)
Gold/copper	Cu (50), Au (50)

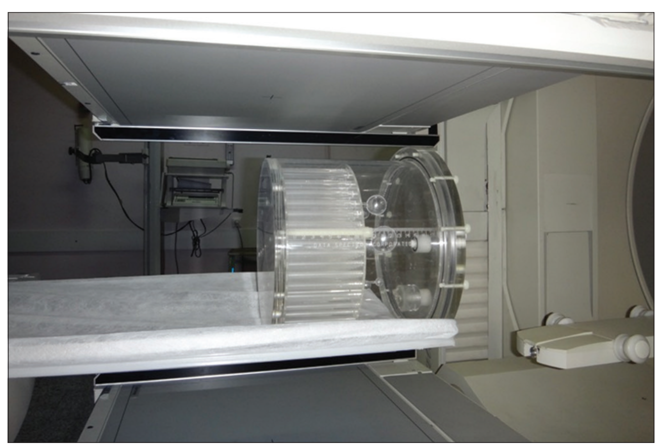

Figure 1: The system setup for Jaszczak scanning by the Siemens E.CAM gamma camera equipped with two removable SE-LEHR collimators

Spatial resolution was obtained by viewing the smallest visible rods for the reconstructed SPECT images of the Jaszczak phantom. The smallest cold rods observed were 9.5 mm in diameter for both the systems. Verification of the simulated system was previously described in detail by Bahreyni Toossi *et al*.[15]

$$\text{Contrast}_{cold}=1-(M\_sp/M\_cy) \quad \text{Eq. 1}$$

where, M_{sp} and M_{cy} correspond to the minimum pixel value in cold spheres and the maximum pixel value in the phantom cylinder, respectively.

Afterward, following a change in the collimator materials, the functional parameters such as sensitivity, energy resolution, spatial resolution or rather the FWHMs of PSF curves were measured for the 17 collimators [Table 3]. The collimator characteristics parameters such as septal penetration and the ratio of the scattered-to-primary photons in the photopeak energy windows were investigated and also the imaging parameters were evaluated by comparing the contrast of Jaszczak phantom cold sphere with 19.1 mm in diameter [Table 4]. We have chosen the 19.1 mm sphere because the contrast of the sphere has shown most contrast similarity between the simulation and the experiment systems.

Effect of the collimator materials on the image contrast of the phantom is shown in Figure 3. According to Table 4, platinum has, on the one hand, the least penetration but on the other hand, the highest scatter-to-primary ratio in the energy windows. There was also a reduction in the sensitivity for the collimator material according to Table 3. According to Tables 3 and 4, the best spatial

Table 2: Results for calculated contrast of cold spheres of Jaszczak phantom from reconstructed SPECT acquisitions obtained experimentally and by SIMIND simulation

Condition	Size of spheres (mm)					
	9.5	12.7	15.9	19.1	25.4	31.8
Simulation	0.539	0.607	0.689	0.792	0.866	0.921
Experiment	0.516	0.562	0.678	0.788	0.825	0.889

Table 3: The results of functional parameters for a ^{99m}Tc point source scanning by simulated SPECT with different collimator materials

Collimator material	Sensitivity (cps/MBq) ±0.01	Energy resolution (%) ±0.01	FWHM (mm) ±0.01
Lead	74.76	10.14	7.74
Lead antimony (1)	74.92	9.87	7.68
Lead antimony (2)	74.57	10.18	7.76
Lichtenberg's metal	76.29	10.12	7.74
Newton's metal	76.52	10.13	7.71
Rose's metal	76.52	10.13	7.74
D'Areet's metal	76.84	10.29	7.76
Solder 1	77.99	10.18	7.84
Solder 2	80.39	10.19	7.90
Malotle's metal	77.90	10.05	7.82
Lipowitz metal (cerrobend)	76.51	10.00	7.82
Wood's metal	76.71	10.13	7.84
Ternary eutectic	79.79	10.00	7.95
Lead_tungsten	74.73	10.04	7.69
Platinum	72.60	10.05	7.71
Platinum-cobalt	73.77	10.03	7.73
Gold/copper	77.99	10.22	7.82

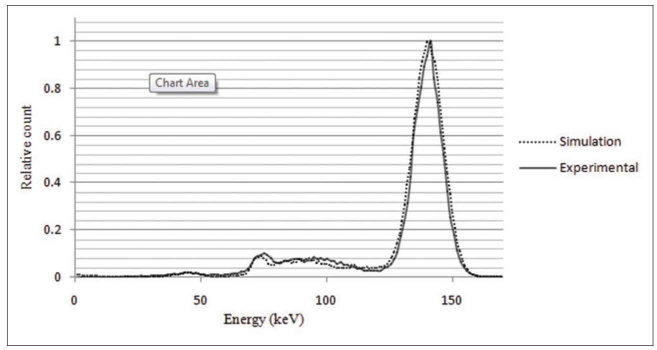

Figure 2: Energy spectra for a ^{99m}Tc point source scanning at 10 cm from the collimator surface with a SPECT system. Related SIMIND simulated spectra (dashed) and experimental energy spectra (solid) are presented

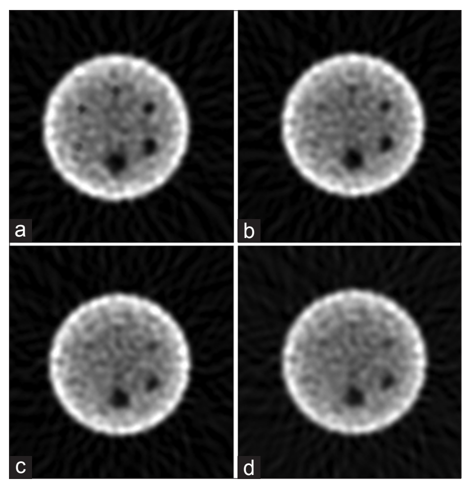

Figure 3: The reconstructed images of cold spheres of simulated Jaszczak phantom filled with 370 MBq ^{99m}Tc that were sorted according to the decreased contrast. The phantom consisting of six cold spheres (the cold rod diameters were 4.8 mm, 6.4 mm, 7.9 mm, 9.5 mm, 11.1 mm, and 12.7 mm). The acquisition parameters were 128 × 128 matrix, 128 projections, 360° clockwise rotation, 1.23 zoom factor, 3.9 mm pixel size, and 1 million counts per projection using a dual-head camera (the Siemens E.CAM gamma camera equipped with two removable SE-LEHR collimators). Images were reconstructed by the FBP with a Butterworth filter of order 5 and cutoff frequency of 0.25 cycles/cm. (a) The best contrast that is related to lead antimony (1) collimator (b) The good contrast achieved by Wood's metal collimator (c) The moderate contrast achieved by lead antimony (2), and finally (d) The poor contrast achieved by gold/copper collimator

Table 4: The results of collimator characteristics parameters for a ^{99m}Tc point source and contrast of 19.1 mm cold sphere of Jaszczak phantom, which were scanned by simulated SPECT with different collimator materials

Collimator material	Penetration (%) ±0.01	Scatter/primary *10-5	Contrast ±0.01
Lead	3.12	2028	0.78
Lead antimony (1)	3.19	2111	0.84
Lead antimony (2)	3.24	2117	0.76
Lichtenberg's metal	4.18	1997	0.73
Newton's metal	4.12	1936	0.82
Rose's metal	4.28	1964	0.73
D'Areet's metal	4.44	1847	0.78
Solder 1	4.99	1813	0.82
Solder 2	6.02	1629	0.78
Malotle's metal	4.97	1851	0.74
Lipowitz metal (cerrobend)	4.27	1920	0.81
Wood's metal	4.38	1905	0.82
Ternary eutectic	5.80	1690	0.76
Lead_tungsten	3.09	2151	0.81
Platinum	1.82	2182	0.81
Platinum-cobalt	2.74	2120	0.80
Gold/copper	4.89	1859	0.72

resolution, energy resolution, and contrast were obtained by the collimator made of 98% lead and 2% antimony [lead antimony (1)] with the best FWHM and energy resolution of 7.68 mm and 9.87%, respectively. It appears that the alloy, as the collimator material, could provide the best image quality in SPECT imaging. It should also be noted that there is always a trade-off between the image resolution and sensitivity in nuclear medicine imaging modality, and the alloy showed a proper spatial resolution from the point of view of the image quality and not sensitivity.

Conclusion

We have used the SIMIND Monte Carlo simulation program to investigate the effect of collimator material on the image and functional parameters in SPECT imaging. The results of our study showed that the LEHR collimator made of 98% lead and 2% antimony offers the best resolution and contrast compared to other high atomic number metals and alloys.

Acknowledgments

The authors are grateful to the head and all the staff members of the nuclear medicine department of Imam Reza Hospital of Tabriz University of Medical Sciences for their sincere cooperation.

Professor Michael Ljungberg has been of great assistance in preparing the files for collimator materials in the simulations. We wish to specially thank him for his assistance. This work was financially supported by the office of the vice president for research in Tabriz University of Medical Sciences, Iran.

References

1. Frangioni JV. New technologies for human cancer imaging. J Clin Oncol 2008;26:4012-21.
2. Khalil MM, Tremoleda JL, Bayomy TB, Gsell W. Molecular SPECT imaging: An overview. Int J Mol Imaging 2011;2011:796025.
3. Bockisch A, Freudenberg LS, Schmidt D, Kuwert T. Hybrid imaging by SPECT/CT and PET/CT: Proven outcomes in cancer imaging. Semin Nucl Med 2009;39:276-89.
4. Coleman RE. Single photon emission computed tomography and positron emission tomography in cancer imaging. Cancer 1991;67(Suppl):1261-70.
5. Islamian JP, Toossi MT, Momennezhad M, Zakavi SR, Sadeghi R, Ljungberg M. Monte carlo study of the effect of collimator thickness on T-99m source response in single photon emission computed tomography. World J Nucl Med 2012;11:70-4.
6. Capote RM, Matela N, Conceição RC, Almeida P. Optimization of convergent collimators for pixelated SPECT systems. Med Phys 2013;40:062501.
7. Lu Y. Collimator Optimization for Single Photon Emission Computed Tomography Using Detection and Localization Tasks. Stony Brook, NY: The Graduate School, Stony Brook University; 2011. p. 1-68.
8. McQuaid SJ, Southekal S, Kijewski MF, Moore SC. Joint optimization of collimator and reconstruction parameters in SPECT imaging for lesion quantification. Phys Med Biol 2011;56:6983-7000.
9. Lee YJ, Ryu HJ, Lee SW, Park SJ, Kim HJ. Comparison of ultra-high-resolution parallel-hole collimator materials based on the CdTe pixelated semiconductor SPECT system. Nucl Instr Meth Phys Res 2013;713:33-9.
10. Lee YJ, Kim DH, Kim HJ. The effect of high-resolution parallel-hole collimator materials with a pixelated semiconductor SPECT system at equivalent sensitivities: Monte Carlo simulation studies. J Korean Phys Soc 2014;64:1055-62.
11. Rajaee A, Shahriari M, Asl AK, Hosseini SH. Simulation study of the influence of collimator material on image quality improvement for high energy photons in nuclear medicine using MCNP code. J Theor Appl Phys 2011;4:13-8.
12. Kurudirek M, Büyükyıldız M, Özdemir Y. Effective atomic number study of various alloys for total photon interaction in the energy region of 1 keV-100 GeV. Nucl Instr Meth Phys Res 2010;613:251-6.
13. Ljungberg M, Strand SE. A Monte Carlo program for the simulation of scintillation camera characteristics. Comput Methods Programs Biomed 1989;29:257-72.
14. Ljungberg M, Strand S-E, King MA. Monte Carlo calculations in nuclear medicine: Appl diagn imaging 2012;1:111-30.
15. Bahreyni Toossi MT, Islamian JP, Momennezhad M, Ljungberg M, Naseri SH. SIMIND Monte Carlo simulation of a single photon emission CT. J Med Phys 2010;35:42-7.
16. Islamian JP, Toossi MT, Momennezhad M, Naseri S, Ljungberg M. Simulation of a quality control jaszczak phantom with SIMIND Monte Carlo and adding the phantom as an accessory to the program. Iranian J Med Phys 2012;9:135-40.
17. Groch MW, Erwin WD. Single-photon emission computed tomography in the year 2001: Instrumentation and quality

control. J Nucl Med Technol 2001;29:12-8.

18. Busemann Sokole E, Płachcínska A, Britten A, Lyra Georgosopoulou M, Tindale W, Klett R. Routine quality control recommendations for nuclear medicine instrumentation. Eur J Nucl Med Mol Imaging 2010;37:662-71.
19. Holstensson M, Hindorf C, Ljungberg M, Partridge M, Flux GD. Optimization of energy-window settings for scatter correction in quantitative (111)In imaging: Comparison of measurements and Monte Carlo simulations. Cancer Biother Radiopharm 2007;22:136-42.

How to cite this article: Azarm A, Islamian JP, Mahmoudian B, Gharepapagh E. The Effect of Parallel-hole Collimator Material on Image and Functional Parameters in SPECT Imaging: A SIMIND Monte Carlo Study. World J Nucl Med 2015;14:160-4.

Source of Support: Nil. **Conflict of Interest:** None declared.